

## Favored configurations for four-quasiparticle $K$ isomerism in the heaviest nuclei

H. L. Liu,<sup>1,\*</sup> P. M. Walker,<sup>2</sup> and F. R. Xu<sup>3</sup>

<sup>1</sup>*Department of Applied Physics, School of Science, Xi'an Jiaotong University, Xi'an 710049, China*

<sup>2</sup>*Department of Physics, University of Surrey, Guildford, Surrey GU2 7XH, UK*

<sup>3</sup>*State Key Laboratory of Nuclear Physics and Technology, School of Physics, Peking University, Beijing 100871, China*

(Received 19 February 2014; published 4 April 2014)

Configuration-constrained potential-energy-surface calculations are performed including  $\beta_6$  deformation to investigate high- $K$  isomeric states in nuclei around  $^{254}\text{No}$  and  $^{270}\text{Ds}$ , the heaviest nuclei where there have been some observations of two-quasiparticle isomers, while data for four-quasiparticle isomers are scarce. We predict the prevalent occurrence of four-quasiparticle isomeric states in these nuclei, together with their favored configurations. The most notable examples, among others, are  $K^\pi = 20^+$  states in  $^{266,268}\text{Ds}$  and  $^{268,270}\text{Cn}$  having very high  $K$  value, relatively low excitation energy, and well-deformed axially symmetric shape. The predicted isomeric states, with hindered spontaneous fission and  $\alpha$  decay, could play a significant role in the future study of superheavy nuclei.

DOI: [10.1103/PhysRevC.89.044304](https://doi.org/10.1103/PhysRevC.89.044304)

PACS number(s): 23.35.+g, 21.60.-n, 23.20.Lv, 27.90.+b

One of the important endeavors in current nuclear-structure studies is to extend the nuclide landscape towards the predicted island of stability of superheavy nuclei and beyond, which will provide us with knowledge about the end of the periodic table of elements, the heaviest magic numbers in nuclei, and the nuclear mass limit [1,2]. When going far away from  $^{208}\text{Pb}$  towards the expected superheavy doubly magic nucleus, nuclear shape significantly deviates from spherical symmetry. The nuclei around  $^{254}\text{No}$  and  $^{270}\text{Ds}$  are predicted to be well deformed with non-negligible higher-order deformation such as  $\beta_6$  [3–6]. Modern spectroscopy experiments (see Refs. [7–9] and references therein) have been able to study these nuclei in detail. Together with various model calculations (see, e.g., Refs. [10–27]), such studies of collective and single-particle excitations result in not only insights into these nuclei themselves but also information for the heavier unknown nuclei due to the contributions of higher-lying single-particle states. Amongst them, multi-quasiparticle (multi-qp) isomers associated with axial symmetry and nearly pure Nilsson configurations provide structure information in a very direct way.

This type of isomer [28] occurs in axially deformed nuclei through unpaired nucleons occupying single-particle states with high- $\Omega$  values ( $\Omega$  is the single-particle angular momentum projection onto the symmetry axis). The total angular momentum along the symmetry axis,  $K$ , is therefore high, and leads to retardation in  $\gamma$ -ray transitions to low- $K$  states. Since the conservation of the  $K$  quantum number is intimately related to axial symmetry, the observations of high- $K$  isomers in nuclei around  $^{254}\text{No}$  and  $^{270}\text{Ds}$  [7] support the predictions of well-developed prolate deformations for the nuclei. These nuclei, with high- $\Omega$  orbitals around the Fermi surfaces for both neutrons and protons, are analogous to the  $A \approx 180$  nuclei and neutron-rich Hf nuclei where not only two-qp but also four-qp (or more) high- $K$  isomers prevail [29–31]. Indeed, it has been observed in  $^{254}\text{No}$  that there exists

a 184  $\mu\text{s}$  2.93 MeV isomer with two unpaired neutrons and two unpaired protons coupled to  $K^\pi = 16^+$  or  $14^+$  [32–36].

The 2.93 MeV isomer in  $^{254}\text{No}$  is so far the unique four-qp isomer known in transfermium nuclei. More could be found with the advance of experimental techniques applicable to the heaviest nuclei. By virtue of their increased number of unpaired nucleons, the four-qp isomers can offer more clues regarding single-particle states in the heavier-mass region [32,33]. The very heavy isomers can be susceptible to spontaneous fission and  $\alpha$  decay besides  $\gamma$ -ray transitions to lower-lying states. The additional decay modes can serve as extra probes into the isomer structure, and the  $\alpha$  decay of an even-even isomer with high angular momentum can populate highly excited states of the daughter nucleus for detailed study. However, the formation of a four-qp isomer is more complex than a two-qp one because of the higher level density accompanying the higher excitation energy. In general, only the lowest one in energy becomes an isomer due to the gap in  $K$  values relative to the lower-lying states. This provides a more stringent testing ground for nuclear models extrapolated to the superheavy-mass region once experimental data are available.

We investigate high- $K$  isomeric states in the heaviest-mass region using configuration-constrained calculations [26,37] of potential-energy surfaces (PESs). The model employs the axially symmetric Woods–Saxon potential [38] with the set of universal parameters [39] to generate single-particle levels. Pairing correlations are treated by the Lipkin–Nogami method [40] with the pairing strength determined by the average gap method [41]. Such treatment with particle numbers approximately conserved can reduce the unphysical fluctuation of the weakened pairing field due to the blocking effect of unpaired nucleons. The unpaired nucleon orbitals that specify a given configuration are traced on the basis of their average Nilsson quantum numbers and then blocked in the pairing calculations at each point of a selected deformation lattice, thus applying a configuration constraint [26,37]. The total energy of a configuration consists of a macroscopic part obtained from the standard liquid-drop model [42] and a microscopic part computed with the Strutinsky shell-correction approach [43],

\*hlliu@mail.xjtu.edu.cn

including blocking effects. Finally, the deformation, excitation energy, and pairing property of a multi-qp state are obtained from the PES minimum, which properly treats the shape changes due to unpaired nucleons.

A three-dimensional deformation space ( $\beta_2$ ,  $\beta_4$ ,  $\beta_6$ ) is adopted in this work to calculate the nuclei of interest. The shape is restricted to be axially symmetric due to the negligible triaxial deformations showing in the calculations with triaxiality [25,26,44]. The  $\beta_6$  degree of freedom is included because of its important role in these nuclei such as the influence on the deformed shell gaps at  $N = 152$  and  $Z = 100$  [3,4], the  $K$ -isomer excitation energy [26], and the angular-momentum alignment in collective rotation [27]. The  $\beta_8$  deformation is omitted because it is calculated to be close to zero. As discussed in Ref. [26], our resulting deformations are slightly different from those obtained by Muntian *et al.* using the Yukawa-plus-exponential model for the macroscopic energy [5]. We perform calculations for the nuclei around  $^{254}\text{No}$  and  $^{270}\text{Ds}$  without adjustment of any parameters.

Figure 1 displays the calculated excitation energies of two-qp high- $K$  states for Fm, No, and Rf isotopes. The excitation energies of each proton two-qp configuration along the isotopic chain remain almost constant as the proton single-particle states are barely influenced by the slight change of neutron number. For the neutron two-qp states, the excitation energies vary dramatically with neutron number, with minima appearing when the neutron Fermi surface is between the two orbitals. Rapid changes in the excitation energies can be seen from  $N = 150$  to 152 nuclei, which reflects the sizable deformed shell gap at  $N = 152$ .

The calculations for  $^{254}\text{No}$  indicate that the close-lying  $\pi^2 8^-$  and  $\nu^2 8_2^-$  states are candidates for the observed two-qp isomer, which we have discussed in Ref. [26] using the same model. It should be mentioned that the  $\nu^2 8_2^-$  coupling is energetically unfavored due to the residual spin-spin interaction between quasiparticles. This effect is not included in our presented energies. The interaction leads to splitting of the spin-antiparallel coupling and the spin-parallel coupling. The former is usually lower in energy for two quasineutrons or two quasiprotons, while it is higher in energy for the configuration

with a quasineutron and a quasiproton, which is known as the Gallagher–Moszkowski (GM) rule [45,46]. In the  $A \approx 180$  mass region, the splitting energy is in the range of  $\approx 100$  to 400 keV [47]. Since the energy correction is small, the  $\pi^2 8^-$  and  $\nu^2 8_2^-$  states in  $^{254}\text{No}$  remain close even taking into account the effect of the residual interaction. In some of the literature (see, e.g., Ref [34]), however, the  $\nu^2 8_2^-$  state is excluded, based on the shell gap at  $N = 152$  that separates the  $\nu 7/2^+$ [613] and  $\nu 9/2^-$ [734] orbitals. The Woods–Saxon potential gives 1.13 MeV for the energy difference between the two orbitals, which is indeed much larger than the 0.63 MeV between the  $\pi 7/2^-$ [514] and  $\pi 9/2^+$ [624] orbitals of the  $\pi^2 8^-$  configuration. However, a quasiparticle energy depends on not only the single-particle levels but also the pairing gap. The latter for the  $\nu^2 8_2^-$  state is smaller than for the  $\pi^2 8^-$  state due to the  $N = 152$  shell gap. As a consequence, the two configurations can have close excitation energies. It is worth noting that the most recent experiment [36] favors neutron character for the observed  $K^\pi = 8^-$  isomer, in contrast to the previous suggestion of the  $\pi^2 8^-$  configuration [32,33,35].

The  $K^\pi = 8^-$  isomer is not likely to occur in neighboring isotone  $^{252}\text{Fm}$ , as shown in Fig. 1. A  $K^\pi = 7^-$  state with the configuration  $\pi 7/2^+$ [633]  $\otimes$   $\pi 7/2^-$ [514] has lower excitation energy than the  $\nu^2 8_2^-$  state. The  $K^\pi = 7^-$  isomeric state seems to also occur in more neutron-rich Fm isotopes (see Fig. 1). Indeed, a 70 ns isomer has been observed in  $^{256}\text{Fm}$  with this configuration suggested [48]. In the  $N = 152$  isotone  $^{256}\text{Rf}$ , signals of high- $K$  isomers were detected but the observations in different experiments are inconsistent [49,50]. Our calculations show that right below the  $\pi^2 8^-$  state there exists an isomeric  $K^\pi = 5^-$  state formed by  $\pi 1/2^-$ [521]  $\otimes$   $\pi 9/2^+$ [624]. A recent experiment observed a three-qp  $K^\pi = 21/2^+$  isomer in neighboring  $^{257}\text{Rf}$  that was suggested to result from the odd neutron at  $11/2^-$ [725] coupled with the  $\pi^2 5^-$  configuration [9]. This points to the occurrence of the  $K^\pi = 5^-$  isomer in  $^{256}\text{Rf}$ .

The situation is less complex in  $N = 150$  and  $N = 148$  isotones where, as shown in Fig. 1, the  $\nu^2 8_1^-$  and  $\nu^2 6^+$  isomeric states systematically occur, respectively. This is consistent with the unambiguous assignment of the  $\nu 7/2^+$ [624]  $\otimes$

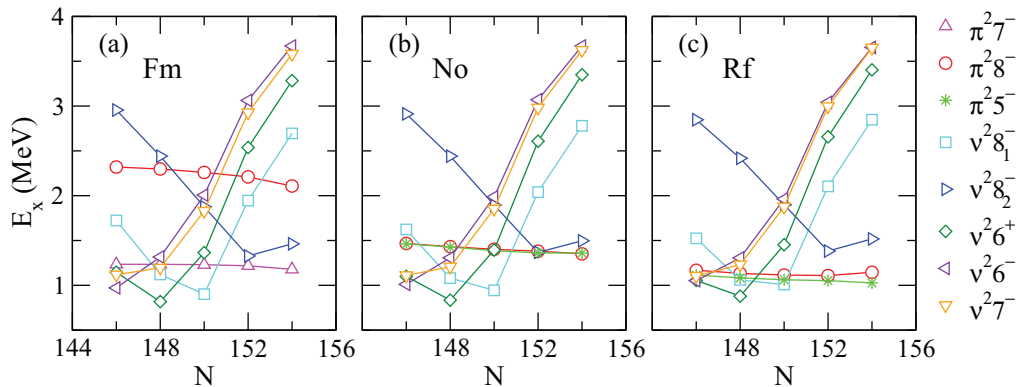


FIG. 1. (Color online) Calculated excitation energies for two-qp high- $K$  states in Fm, No, and Rf nuclei ( $Z = 100, 102$ , and  $104$ ). Configurations:  $\pi^2 7^-$  ( $\pi 7/2^+$ [633]  $\otimes$   $\pi 7/2^-$ [514]),  $\pi^2 8^-$  ( $\pi 7/2^-$ [514]  $\otimes$   $\pi 9/2^+$ [624]),  $\pi^2 5^-$  ( $\pi 1/2^-$ [521]  $\otimes$   $\pi 9/2^+$ [624]),  $\nu^2 8_1^-$  ( $\nu 7/2^+$ [624]  $\otimes$   $\nu 9/2^-$ [734]),  $\nu^2 8_2^-$  ( $\nu 7/2^+$ [613]  $\otimes$   $\nu 9/2^-$ [734]),  $\nu^2 6^+$  ( $\nu 5/2^+$ [622]  $\otimes$   $\nu 7/2^+$ [624]),  $\nu^2 6^-$  ( $\nu 7/2^-$ [743]  $\otimes$   $\nu 5/2^+$ [622]),  $\nu^2 7^-$  ( $\nu 7/2^-$ [743]  $\otimes$   $\nu 7/2^+$ [624]).

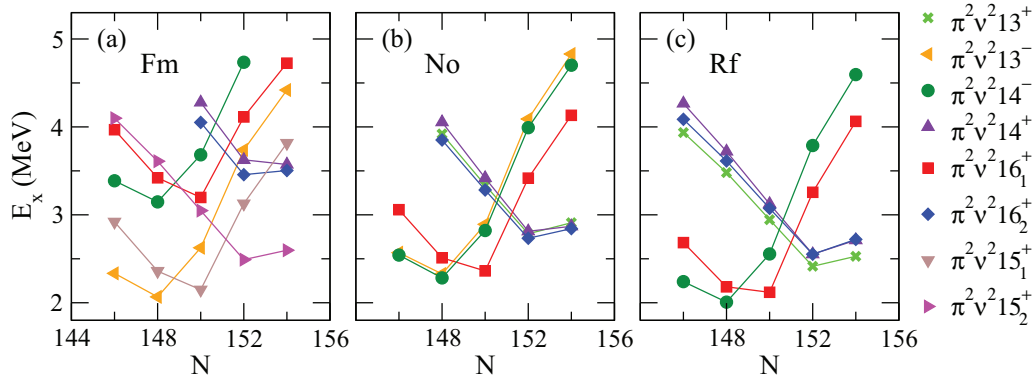


FIG. 2. (Color online) Calculated excitation energies for four-qp high- $K$  states in Fm, No, and Rf nuclei. Configurations:  $\pi^2\nu^213^+(\pi^25^- \otimes \nu^28_2^-)$ ,  $\pi^2\nu^213^-(\pi^27^- \otimes \nu^26^+)$ ,  $\pi^2\nu^214^-(\pi^28^- \otimes \nu^26^+)$ ,  $\pi^2\nu^214^+(\pi^28^- \otimes \nu^3/2^+[622] \otimes \nu^9/2^-[734])$ ,  $\pi^2\nu^216_1^+(\pi^28^- \otimes \nu^28_1^-)$ ,  $\pi^2\nu^216_2^+(\pi^28^- \otimes \nu^28_2^-)$ ,  $\pi^2\nu^215_1^+(\pi^27^- \otimes \nu^28_1^-)$ ,  $\pi^2\nu^215_2^+(\pi^27^- \otimes \nu^28_2^-)$ .

$\nu^9/2^-[734]$  configuration to the observed  $K^\pi = 8^-$  isomers in  $^{250}\text{Fm}$  [51] and  $^{252}\text{No}$  [52] through measuring  $B(M1)/B(E2)$  ratios. Our calculated excitation energies are 0.90 MeV for the  $^{250}\text{Fm}$  isomer and 0.94 MeV for the  $^{252}\text{No}$  isomer, compared to the measured data of 1.20 and 1.25 MeV [7], respectively. The underestimation of the calculations could be improved with the pairing strength adjusted by fitting experimental odd-even mass differences [37] which, however, cannot be generally performed in this region due to scarce mass data. The  $\nu^28_1^-$  state is still the lowest-lying high- $K$  state in  $^{254}\text{Rf}$ , indicating the formation of an isomer. For the  $N = 148$  isotones, a fissioning isomer was observed in  $^{250}\text{No}$  [53] with the configuration  $\nu^5/2^+[622] \otimes \nu^7/2^+[624]$  suggested. This  $\nu^26^+$  configuration was also tentatively proposed for the 10.1 ms isomer in  $^{248}\text{Fm}$  observed with low statistics (see Ref. [54] and reference therein). Our calculations support these configuration suggestions and predict the  $\nu^26^+$  state to be also isomeric in  $^{252}\text{Rf}$  (see Fig. 1).

The calculations for four-qp high- $K$  states in Fm, No, and Rf isotopes are presented in Fig. 2 where one can see the favored configuration for isomerism, i.e., the lowest-lying one in each nucleus. So far only one four-qp isomer has

been observed in transfermium nuclei, which is the 184  $\mu\text{s}$  2.93 MeV state in  $^{254}\text{No}$  [32–36]. We have discussed this isomer in detail in Ref. [26] with its configuration suggested to be  $\pi^2\nu^216_2^+$ , which is consistent with the  $K^\pi = 16^+$  assignment in the most recent experiment [36]. The state is formed by the coupling of the two lowest-lying high- $K$  configurations  $\pi^28^-$  and  $\nu^28_2^-$ . Similar couplings lead to the occurrence of four-qp isomeric states in neighboring nuclei (see Fig. 2). The  $\pi^2\nu^216_1^+$  state in  $^{252}\text{No}$  and  $^{254}\text{Rf}$  originates from  $\pi^28^- \otimes \nu^28_1^-$  which is well separated from other four-qp states, clearly indicating isomeric character. The isomeric states are calculated to have excitation energies of 2.36 and 2.12 MeV for  $^{252}\text{No}$  and  $^{254}\text{Rf}$ , respectively. In the  $N = 148$  isotones  $^{250}\text{No}$  and  $^{252}\text{Rf}$ , the  $\pi^28^-$  configuration combined with the  $\nu^26^+$  configuration results in the  $K^\pi = 14^-$  isomeric state. The isomeric states in Fm isotopes appear with the participation of the  $\pi^27^-$  configuration, instead of the  $\pi^28^-$  configuration that lies high in energy. Our calculations thus indicate the prevalence of four-qp isomeric states in the nuclei around  $^{254}\text{No}$ . Similar results were obtained by Kondev *et al.* [34], who included the effects of residual spin-spin interactions but did not allow different excited states to have different deformations. In both

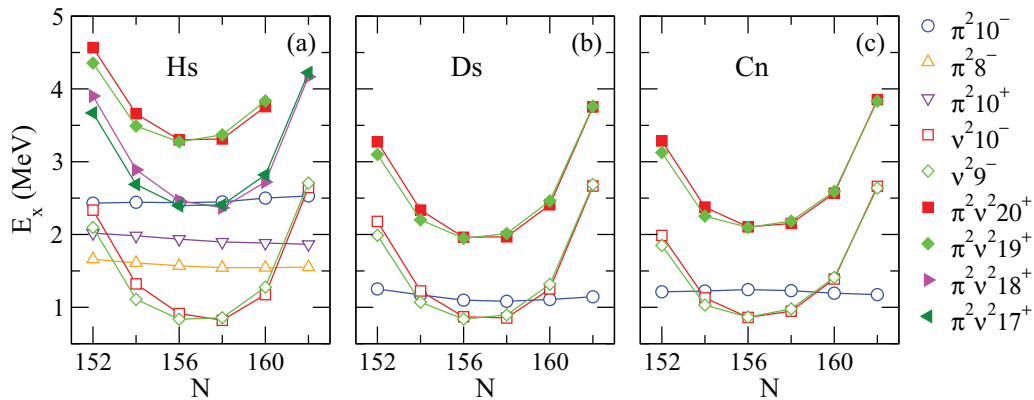


FIG. 3. (Color online) Calculated excitation energies for two- and four-qp high- $K$  states in Hs, Ds, and Cn nuclei ( $Z = 108, 110, \text{ and } 112$ ). Configurations:  $\pi^210^-(\pi^9/2^-[505] \otimes \pi^11/2^+[615])$ ,  $\pi^28^-(\pi^5/2^-[512] \otimes \pi^11/2^+[615])$ ,  $\pi^210^+(\pi^9/2^+[624] \otimes \pi^11/2^+[615])$ ,  $\nu^210^-(\nu^9/2^+[615] \otimes \nu^11/2^-[725])$ ,  $\nu^29^-(\nu^7/2^+[613] \otimes \nu^11/2^-[725])$ ,  $\pi^2\nu^220^+(\pi^210^- \otimes \nu^210^-)$ ,  $\pi^2\nu^219^+(\pi^210^- \otimes \nu^29^-)$ ,  $\pi^2\nu^218^+(\pi^28^- \otimes \nu^210^-)$ ,  $\pi^2\nu^217^+(\pi^28^- \otimes \nu^29^-)$ .

sets of calculations, it is notable that the  $N = 150$  isotones  $^{252}\text{No}$  and  $^{254}\text{Rf}$  have especially favored  $K^\pi = 16^+$  states, indicating that unusually long half-lives are to be expected.

For heavier nuclei around  $^{270}\text{Ds}$ , the Fermi surfaces move to the upper parts of high- $j$  orbitals, with high- $\Omega$  values such as  $\nu 11/2^-$  [725],  $\nu 9/2^+$  [615],  $\nu 7/2^+$  [613],  $\pi 11/2^+$  [615], and  $\pi 9/2^-$  [505]. This favors the formation of isomeric states with very high  $K$  values and relatively low excitation energies, as shown in Fig. 3. Experiment has observed an  $\alpha$ -decaying isomer with  $E_x \simeq 1.13$  MeV in  $^{270}\text{Ds}$  with suggested configuration  $\nu^2 10^-$  or  $\nu^2 9^-$  [7,56,57]. The present calculations, with higher-order deformation  $\beta_6$  included, give three close-lying states  $\pi^2 10^-$  ( $E_x = 1.11$  MeV),  $\nu^2 10^-$  ( $E_x = 1.25$  MeV), and  $\nu^2 9^-$  ( $E_x = 1.32$  MeV) in  $^{270}\text{Ds}$ , similar to the results in Ref. [25]. Here the  $\beta_6$  deformation is smaller than in Fm, No, and Rf nuclei. For instance,  $\beta_6 = -0.012$  is obtained for the  $^{270}\text{Ds}$   $\pi^2 10^-$  state, compared to  $-0.024$  for the  $^{254}\text{No}$   $\nu^2 8_2^-$  state. The  $\alpha$  decay of the  $^{270}\text{Ds}$  isomer populates excited states in  $^{266}\text{Hs}$ , one of which was found to be an isomer in a later experiment [56]. The isomer is likely the  $\nu^2 10^-$  or  $\nu^2 9^-$  state that are very close in energy in our calculations (see Fig. 3). The  $\nu^2 10^-$  configuration is more probable because of its favored coupling in energy in contrast to the energetically unfavored coupling  $\nu^2 9^-$ , according to the GM rule [45,46]. In fact, the  $\nu^2 10^-$  configuration has the lowest excitation energies at  $N = 156, 158$  in Hs, Ds, and Cn isotopes. Its coupling with the proton two-qp configuration  $\pi^2 10^-$  can form isomeric states with  $K^\pi = 20^+$ , which is higher in angular momentum than any other four-qp  $K$  value known to date. Furthermore, their calculated excitation energies are as low as  $\approx 2$  MeV for  $^{266,268}\text{Ds}$  and  $^{268,270}\text{Cn}$ , favoring strong  $K$  hindrance [58] and long half-lives. It is interesting to compare these isomeric states with the predicted  $K^\pi = 18^+$  isomeric state in neutron-rich  $^{188}\text{Hf}$  that could also be long lived [28,29,31]. The isomerism in the latter with  $\beta_2 < 0.2$ , however, could be affected by softness against triaxiality that leads to  $K$  mixing, as discussed in Ref. [31]. For the nuclei around  $^{270}\text{Ds}$ , the calculated deformation is  $\beta_2 \approx 0.22$ , only slightly less deformed compared to the nuclei around  $^{254}\text{No}$  with  $\beta_2 \approx 0.25$ . Note that the observed isomer in  $^{270}\text{Ds}$  has a half-life of  $3.9_{-0.8}^{+1.3}$  ms which is much longer than the ground-state half-life of  $0.20_{-0.04}^{+0.07}$  ms [56,57], implying a well-deformed axially symmetric shape that leads to good conservation of the  $K$  quantum number. The  $K^\pi = 20^+$  states in  $^{266,268}\text{Ds}$  and  $^{268,270}\text{Cn}$ , with favored conditions for isomerism in terms of  $K$  value, excitation energy, and deformation, could provide extreme examples of  $K$  isomers.

The very heavy  $K$  isomers can decay via spontaneous fission. For example, it was observed that the decay of the  $K^\pi = 6^+$  isomer in  $^{250}\text{No}$  is associated with a fission activity having a half-life of  $43_{-15}^{+22}$   $\mu\text{s}$ , which is longer than that of the ground state at  $3.7_{-0.8}^{+1.1}$   $\mu\text{s}$  [53]. This ‘‘inversion’’ of stability indicates the significant role of high- $K$  isomerism in the study of superheavy nuclei, as pointed out in Ref. [25]. The increased hindrance in fission of multi-qp states can be attributed to the reduced superfluidity and increased fission barrier due to unpaired nucleons. In general, the fission barrier of a multi-qp state is higher and wider than that of the corresponding ground state in our configuration-constrained PES calculations

[25,26,44,59]. It is found that the  $\beta_6$  deformation contributes to the increased fission barrier height [26,59].

The very heavy  $K$  isomers can decay via  $\alpha$  emission as well, such as the afore-mentioned isomer in  $^{270}\text{Ds}$  with its notably long lifetime. Its enhanced stability against  $\alpha$  decay is partly ascribed to the increased difficulty in  $\alpha$ -particle preformation due to the unpaired nucleons (see Ref. [25]). In Fig. 4, the calculated  $Q_\alpha$  values for the ground and isomeric states decaying to the same configuration of the daughter nuclide are compared with available experimental data. The ground-state results are in good agreement with the data. Our calculations of  $^{270}\text{Ds}$  with  $\beta_6$  deformation give  $Q_\alpha = 11.45$  MeV for the  $\nu^2 10^-$  state and  $Q_\alpha = 9.69$  MeV for the  $\pi^2 10^-$  state. For the decay of the  $\pi^2 10^-$  isomeric state in  $^{270}\text{Ds}$  to the  $\nu^2 10^-$  isomeric state in  $^{266}\text{Hs}$ ,  $Q_\alpha$  is calculated to be 11.31 MeV, in agreement with the newly measured value 11.13 MeV for the isomer [56]. It is worth noting that the calculated  $Q_\alpha$  values of the four-qp isomeric states in No (Ds) isotopes are generally smaller than in Rf (Cn) isotopes. This is because the configuration in the No parent nuclide has significantly lower excitation energy than in the Fm daughter nuclide, while the same configurations in each Rf-No parent-daughter pair have similar excitation energies (see Fig. 2). The same situation happens in Hs, Ds, and Cn nuclei, as shown in Fig. 3. Since the  $\alpha$ -decay half-life increases quickly with decreasing decay energy, it seems more difficult for the four-qp isomeric states in No (Ds) nuclei to undergo  $\alpha$  decay than in Rf (Cn) nuclei. The details of our calculations for the isomeric states are summarized in Table I.

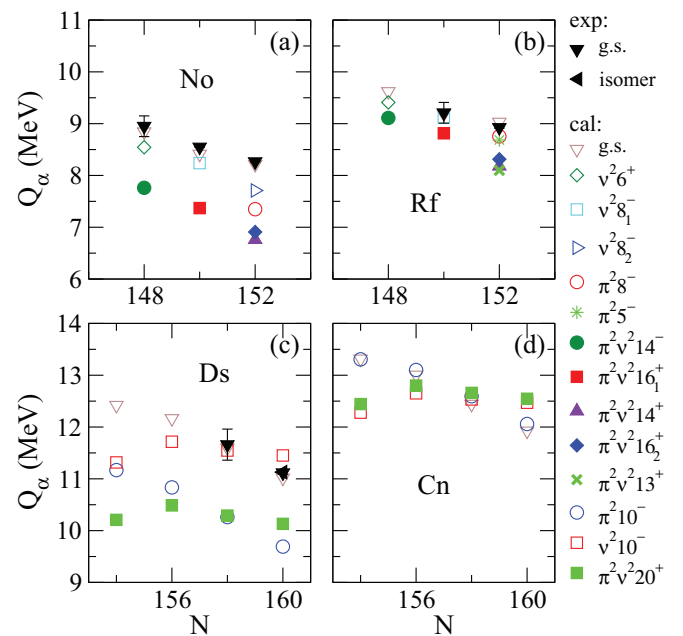


FIG. 4. (Color online) Calculated and experimental  $Q_\alpha$  values for ground and isomeric states decaying to the same configuration in the daughter nucleus. Experimental data for ground states are taken from Ref. [55]; that for the isomer in  $^{270}\text{Ds}$  from Ref. [56]. See text for the comparison of calculated and measured  $Q_\alpha$  values for the  $^{270}\text{Ds}$  isomer. The data error bar cannot be seen if it is shorter than the size of the symbol.

TABLE I. Calculated ground- and isomeric-state deformations, excitation energies, and  $Q_\alpha$  values for the decay to the same configuration of the daughter nucleus. Experimental data are taken from Refs. [7,55]. See text for the comparison of calculated and measured  $Q_\alpha$  values for the  $^{270}\text{Ds}$  isomer.

Nucleus	Config.	$\beta_2$	$\beta_4$	$\beta_6$	$E_x$ (MeV)		$Q_\alpha$ (MeV)	
					Calc.	Expt.	Calc.	Expt.
$^{250}\text{No}$	g.s.	0.24	0.030	-0.024			8.84	8.95
	$\nu^2 6^+$	0.24	0.032	-0.024	0.83		8.55	
	$\pi^2 \nu^2 14^-$	0.24	0.029	-0.023	2.28		7.76	
$^{252}\text{No}$	g.s.	0.25	0.020	-0.026			8.41	8.55
	$\nu^2 8_1^-$	0.25	0.023	-0.027	0.94	1.25	8.24	
	$\pi^2 \nu^2 16_1^+$	0.24	0.020	-0.026	2.36		7.37	
$^{254}\text{No}$	g.s.	0.25	0.011	-0.029			8.22	8.27
	$\nu^2 8_2^-$	0.24	0.012	-0.024	1.37	1.29	7.71	
	$\pi^2 8^-$	0.25	0.009	-0.028	1.38		7.35	
	$\pi^2 \nu^2 16_2^+$	0.24	0.010	-0.024	2.73	2.93	6.91	
	$\pi^2 \nu^2 14^+$	0.25	0.008	-0.028	2.81		6.76	
$^{252}\text{Rf}$	g.s.	0.24	0.018	-0.023			9.62	
	$\nu^2 6^+$	0.24	0.022	-0.023	0.88		9.41	
	$\pi^2 \nu^2 14^-$	0.25	0.020	-0.028	2.01		9.11	
$^{254}\text{Rf}$	g.s.	0.24	0.009	-0.026			9.19	9.21
	$\nu^2 8_1^-$	0.25	0.013	-0.026	1.01		9.12	
	$\pi^2 \nu^2 16_1^+$	0.25	0.012	-0.030	2.12		8.81	
$^{256}\text{Rf}$	g.s.	0.25	0.001	-0.028			9.03	8.93
	$\pi^2 5^-$	0.24	-0.001	-0.027	1.05		8.69	
	$\pi^2 8^-$	0.25	0.001	-0.032	1.11		8.75	
	$\pi^2 \nu^2 13^+$	0.24	0.000	-0.023	2.42		8.10	
$^{264}\text{Ds}$	g.s.	0.23	-0.026	-0.020			12.42	
	$\pi^2 10^-$	0.22	-0.025	-0.019	1.17		11.17	
	$\nu^2 10^-$	0.23	-0.025	-0.017	1.22		11.32	
	$\pi^2 \nu^2 20^+$	0.22	-0.025	-0.017	2.34		10.21	
$^{266}\text{Ds}$	g.s.	0.23	-0.036	-0.016			12.17	
	$\nu^2 10^-$	0.23	-0.036	-0.016	0.87		11.72	
	$\pi^2 \nu^2 20^+$	0.22	-0.034	-0.016	1.96		10.49	
$^{268}\text{Ds}$	g.s.	0.22	-0.046	-0.014			11.60	11.66
	$\nu^2 10^-$	0.23	-0.047	-0.015	0.85		11.55	
	$\pi^2 \nu^2 20^+$	0.22	-0.043	-0.015	1.97		10.29	
$^{270}\text{Ds}$	g.s.	0.22	-0.057	-0.011			11.02	11.12
	$\pi^2 10^-$	0.21	-0.052	-0.012	1.11	1.13	9.69	
	$\nu^2 10^-$	0.23	-0.058	-0.014	1.25		11.45	
	$\pi^2 \nu^2 20^+$	0.22	-0.052	-0.015	2.41		10.13	
$^{266}\text{Cn}$	g.s.	0.22	-0.021	-0.016			13.32	
	$\pi^2 10^-$	0.23	-0.023	-0.016	1.22		13.31	
	$\nu^2 10^-$	0.21	-0.022	-0.014	1.13		12.28	
	$\pi^2 \nu^2 20^+$	0.22	-0.024	-0.014	2.38		12.44	
$^{268}\text{Cn}$	g.s.	0.21	-0.032	-0.012			13.00	
	$\nu^2 10^-$	0.21	-0.032	-0.012	0.86		12.65	
	$\pi^2 \nu^2 20^+$	0.22	-0.036	-0.012	2.11		12.80	
$^{270}\text{Cn}$	g.s.	0.21	-0.044	-0.009			12.44	
	$\nu^2 10^-$	0.21	-0.046	-0.011	0.95		12.53	
	$\pi^2 \nu^2 20^+$	0.22	-0.048	-0.011	2.15		12.66	
$^{272}\text{Cn}$	g.s.	0.21	-0.056	-0.007			11.93	
	$\pi^2 10^-$	0.21	-0.059	-0.007	1.19		12.06	
	$\nu^2 10^-$	0.22	-0.058	-0.010	1.39		12.47	
	$\pi^2 \nu^2 20^+$	0.22	-0.059	-0.010	2.57		12.55	

In conclusion, high- $K$  isomeric states in nuclei around  $^{254}\text{No}$  and  $^{270}\text{Ds}$  have been investigated by configuration-constrained PES calculations including higher-order deformation  $\beta_6$ . The calculations are consistent with available experimental data and give favored configurations for four-qp isomeric states that are predicted to prevail in these nuclei, besides two-qp ones. In particular, the  $K^\pi = 20^+$  states in  $^{266,268}\text{Ds}$  and  $^{268,270}\text{Cn}$ , with very high  $K$  value, relatively low excitation energy, and well-developed axially symmetric deformation, could be ex-

treme examples of high- $K$  isomers. Experimental observations of the heaviest isomers can also provide valuable clues to the location of the expected superheavy island of stability.

This work is supported by the National Natural Science Foundation of China under Grants No. 11205120, No. 11235001, and No. 11320101004, the National Key Basic Research Program of China under Grant No. 2013CB834400, and the UK STFC.

- 
- [1] S. Hofmann and G. Münzenberg, *Rev. Mod. Phys.* **72**, 733 (2000).
- [2] Yu. Oganessian, *J. Phys. G* **34**, R165 (2007).
- [3] Z. Patyk and A. Sobiczewski, *Nucl. Phys. A* **533**, 132 (1991).
- [4] Z. Patyk and A. Sobiczewski, *Phys. Lett. B* **256**, 307 (1991).
- [5] I. Muntian, Z. Patyk, and A. Sobiczewski, *Phys. Lett. B* **500**, 241 (2001).
- [6] A. Sobiczewski and K. Pomorski, *Prog. Part. Nucl. Phys.* **58**, 292 (2007).
- [7] R.-D. Herzberg and P. T. Greenlees, *Prog. Part. Nucl. Phys.* **61**, 674 (2008).
- [8] P. T. Greenlees *et al.*, *Phys. Rev. Lett.* **109**, 012501 (2012).
- [9] J. Rissanen *et al.*, *Phys. Rev. C* **88**, 044313 (2013).
- [10] I. Muntian, Z. Patyk, and A. Sobiczewski, *Phys. Rev. C* **60**, 041302(R) (1999).
- [11] A. Sobiczewski, I. Muntian, and Z. Patyk, *Phys. Rev. C* **63**, 034306 (2001).
- [12] X.-T. He, Z.-Z. Ren, S.-X. Liu, and E.-G. Zhao, *Nucl. Phys. A* **817**, 45 (2009).
- [13] G. G. Adamian, N. V. Antonenko, and W. Scheid, *Phys. Rev. C* **81**, 024320 (2010).
- [14] Z.-H. Zhang, J.-Y. Zeng, E.-G. Zhao, and S.-G. Zhou, *Phys. Rev. C* **83**, 011304(R) (2011).
- [15] Z.-H. Zhang, X.-T. He, J.-Y. Zeng, E.-G. Zhao, and S.-G. Zhou, *Phys. Rev. C* **85**, 014324 (2012).
- [16] Z.-H. Zhang, J. Meng, E.-G. Zhao, and S.-G. Zhou, *Phys. Rev. C* **87**, 054308 (2013).
- [17] T. Duguet, P. Bonche, and P.-H. Heenen, *Nucl. Phys. A* **679**, 427 (2001).
- [18] M. Bender, P. Bonche, T. Duguet, and P.-H. Heenen, *Nucl. Phys. A* **723**, 354 (2003).
- [19] J. L. Egido and L. M. Robledo, *Phys. Rev. Lett.* **85**, 1198 (2000).
- [20] J.-P. Delaroche, M. Girod, H. Goutte, and J. Libert, *Nucl. Phys. A* **771**, 103 (2006).
- [21] A. V. Afanasjev, T. L. Khoo, S. Frauendorf, G. A. Lalazissis, and I. Ahmad, *Phys. Rev. C* **67**, 024309 (2003).
- [22] A. V. Afanasjev and O. Abdurazakov, *Phys. Rev. C* **88**, 014320 (2013).
- [23] Y.-S. Chen, Y. Sun, and Z.-C. Gao, *Phys. Rev. C* **77**, 061305(R) (2008).
- [24] F. Al-Khudair, G.-L. Long, and Y. Sun, *Phys. Rev. C* **79**, 034320 (2009).
- [25] F. R. Xu, E. G. Zhao, R. Wyss, and P. M. Walker, *Phys. Rev. Lett.* **92**, 252501 (2004).
- [26] H. L. Liu, F. R. Xu, P. M. Walker, and C. A. Bertulani, *Phys. Rev. C* **83**, 011303(R) (2011).
- [27] H. L. Liu, F. R. Xu, and P. M. Walker, *Phys. Rev. C* **86**, 011301(R) (2012).
- [28] P. M. Walker and G. D. Dracoulis, *Nature (London)* **399**, 35 (1999).
- [29] P. M. Walker and G. D. Dracoulis, *Hyperfine Interact.* **135**, 83 (2001).
- [30] M. W. Reed *et al.*, *Phys. Rev. Lett.* **105**, 172501 (2010).
- [31] H. L. Liu, F. R. Xu, P. M. Walker, and C. A. Bertulani, *Phys. Rev. C* **83**, 067303 (2011).
- [32] R.-D. Herzberg *et al.*, *Nature (London)* **442**, 896 (2006).
- [33] S. K. Tandel *et al.*, *Phys. Rev. Lett.* **97**, 082502 (2006).
- [34] F. G. Kondev *et al.*, in *Proceedings of the International Conference on Nuclear Data for Science and Technology, Nice, France, 2007*, edited by O. Bersillon *et al.* (EDP Sciences, Les Ulis Cedex, France, 2008).
- [35] F. P. Heßberger *et al.*, *Eur. Phys. J. A* **43**, 55 (2010).
- [36] R. M. Clark *et al.*, *Phys. Lett. B* **690**, 19 (2010).
- [37] F. R. Xu, P. M. Walker, J. A. Sheikh, and R. Wyss, *Phys. Lett. B* **435**, 257 (1998).
- [38] S. Ćwiok, J. Dudek, W. Nazarewicz, S. Skalski, and T. Werner, *Comput. Phys. Commun.* **46**, 379 (1987).
- [39] W. Nazarewicz, J. Dudek, R. Bengtsson, T. Bengtsson, and I. Ragnarsson, *Nucl. Phys. A* **435**, 397 (1985).
- [40] H. C. Pradhan, Y. Nogami, and J. Law, *Nucl. Phys. A* **201**, 357 (1973).
- [41] P. Möller and J. R. Nix, *Nucl. Phys. A* **536**, 20 (1992).
- [42] W. D. Myers and W. J. Swiatecki, *Nucl. Phys.* **81**, 1 (1966).
- [43] V. M. Strutinsky, *Nucl. Phys. A* **95**, 420 (1967).
- [44] P. M. Walker, F. R. Xu, H. L. Liu, and Y. Sun, *J. Phys. G* **39**, 105106 (2012).
- [45] C. J. Gallagher and S. A. Moszkowski, *Phys. Rev.* **111**, 1282 (1958).
- [46] C. J. Gallagher, *Phys. Rev.* **126**, 1525 (1962).
- [47] K. Jain *et al.*, *Nucl. Phys. A* **591**, 61 (1995).
- [48] H. L. Hall *et al.*, *Phys. Rev. C* **39**, 1866 (1989).
- [49] H. B. Jeppesen *et al.*, *Phys. Rev. C* **79**, 031303(R) (2009).
- [50] A. P. Robinson *et al.*, *Phys. Rev. C* **83**, 064311 (2011).
- [51] P. T. Greenlees *et al.*, *Phys. Rev. C* **78**, 021303(R) (2008).
- [52] B. Sulignano *et al.*, *Phys. Rev. C* **86**, 044318 (2012).
- [53] D. Peterson *et al.*, *Phys. Rev. C* **74**, 014316 (2006).
- [54] R.-D. Herzberg and D. M. Cox, *Radiochim. Acta* **99**, 441 (2011).
- [55] M. Wang *et al.*, *Chin. Phys. C* **36**, 1603 (2012).
- [56] D. Ackermann *et al.*, *GSI Sci. Rep.* **2011**, 208 (2012).
- [57] S. Hofmann *et al.*, *Eur. Phys. J. A* **10**, 5 (2001).
- [58] P. M. Walker *et al.*, *Phys. Lett. B* **408**, 42 (1997).
- [59] H. L. Liu and F. R. Xu, *Chin. Sci. Bull.* **59**, 11 (2014).